

Realization of spin gapless semiconductors: the Heusler compound Mn_2CoAl .

Siham Ouardi, Gerhard H. Fecher,* and Claudia Felser
Max Planck Institute for Chemical Physics of Solids, D-01187 Dresden, Germany

Jürgen Kübler

Institut für Festkörperphysik, Technische Universität Darmstadt, D-64289 Darmstadt, Germany

(Dated: October 2, 2012)

Recent studies have reported an interesting class of semiconductor materials that bridge the gap between semiconductors and halfmetallic ferromagnets. These materials, called *spin gapless semiconductors*, exhibit a bandgap in one of the spin channels and a zero bandgap in the other and thus allow for tunable spin transport. Here, a theoretical and experimental study of the spin gapless Heusler compound Mn_2CoAl is presented. It turns out that Mn_2CoAl is a very peculiar *ferrimagnetic semiconductor* with a magnetic moment of $2 \mu_B$ and a high Curie temperature of 720 K. Below 300 K, the compound exhibits nearly temperature-independent conductivity, very low, temperature-independent carrier concentration, and a vanishing Seebeck coefficient. The magnetoresistance changes sign with temperature. In high fields, it is positive and non-saturating at low temperatures, but negative and saturating at high temperatures. The anomalous Hall effect is comparatively low, which is explained by the close antisymmetry of the Berry curvature for k_z of opposite sign.

PACS numbers: 03.65.Vf, 71.20.Lp, 71.20.Nr, 72.20.Jv, 72.20.My, 72.25.-b, 75.50.Pp, 85.75.-d

Keywords: Heusler compounds, Halfmetallic ferrimagnets, Spin gapless semiconductors, Anomalous Hall effect, Berry curvature

Recent studies have reported an interesting class of materials, namely *spin gapless* semiconductors [1]. These materials are closely related to halfmetallic ferromagnets [2], the properties of which also bridge the gap between metals and semiconductors. Special cases of halfmetallic materials are halfmetallic ferrimagnets with antiparallel orientation of their magnetic moments. This results in some cases in completely compensated halfmetals [3], which are sometimes termed halfmetallic antiferromagnets [4]. In all halfmetallic materials, transport is mediated by electrons having only one kind of spin, i.e., the minority or majority spin. *Spin gapless* semiconductors exhibit an additional phenomenon, namely an open bandgap in one spin channel and a closed bandgap (*zero bandgap*) in the other. The principal density of states schemes for halfmetallic ferromagnets and spin gapless semiconductors are shown in Figure 1.

In the present example, the Fermi energy intersects the majority density in halfmetallic ferromagnets (Figure 1a)). The class of spin gapless semiconductors appears if the conduction and valence band edges of the majority electrons touch at the Fermi energy ϵ_F (Figure 1b)). This class is thus an important sub-class of *zero bandgap* insulators or *gapless semiconductors* [5]. In zero bandgap materials, no threshold energy is required to move electrons from occupied states to empty states. These materials therefore exhibit unique properties, as their electronic structures are extremely sensitive to external influences [5]. Many of the known gapless semiconductors exhibit a so-called inverted band structure [5, 6], and they act as topological insulators [7, 8], in which the bandgap is re-opened in the presence of a strong spin-

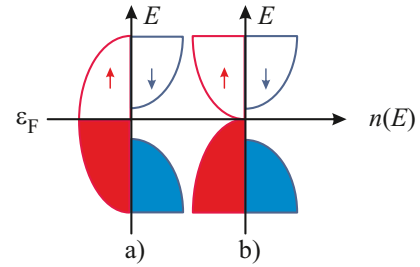


FIG. 1. Density of states schemes.

The schematic density of states $n(E)$ as a function of energy E is shown for a) a halfmetallic ferromagnet and b) a spin gapless semiconductor. The occupied states are indicated by filled areas. Arrows indicate the majority (\uparrow) and minority (\downarrow) states.

orbit (SO) interaction. In *spin gapless* semiconductors, not only the excited electrons but also the holes can be 100% spin polarized. Indeed, the Fermi energy needs to fall inside the majority gap, and it cannot touch the band edges. This results in unique transport properties that can be influenced by the magnetic state of the material or by magnetic fields.

Based on these findings of previous studies, as mentioned above, the Heusler compound Mn_2CoAl was investigated in greater detail, using theoretical and experimental methods, in order to prove the occurrence of spin gapless semiconductivity. The compound crystallizes in the inverse Heusler structure with space group $F\bar{4}3m$ and

Wyckhoff sequence $abcd$ for the atoms Mn-Mn-Co-Al. To explain the electronic structure and magnetic properties, *ab initio* calculations were performed using the augmented spherical wave (ASW) method [9], which is extremely fast and efficient. Berry curvatures were computed using ASW density functional calculations and the wave functions that they provide, allowing the anomalous Hall conductivity to be obtained from the Berry curvatures. The technical details of such calculations have been reported in Reference [10].

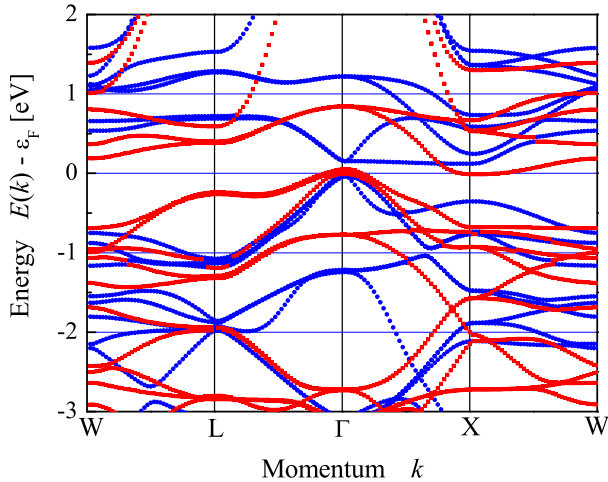


FIG. 2. Band structure of Mn_2CoAl . The band structure calculated with spin-orbit interaction is shown. Majority (red) and minority (blue) spin characters of the bands are distinguished by different colors.

Figure 2 shows the band structure of Mn_2CoAl . The calculations were performed with SO interactions respected for all atoms, as this is essential for the Berry curvature calculations reported below. The electronic structure agrees well with reports of bare spin density functional calculations not respecting SO [11]. In Figure 2, the spin character of the bands is indicated by different colors. The spin character of the bands close to the Fermi energy is pure, even though the SO interaction mixes, in general, states with different spin projections. Obviously, the band structure also exhibits the expected halfmetallic character with a bandgap in the minority states (blue) when the SO interaction is included in the calculations. A most interesting observation is the bandgap that also appears in the majority channel. This is neither a semiconductor nor a halfmetallic ferromagnet, because the indirect gap appears to be just closed as a result of bands touching the Fermi energy at Γ (valence band) and X (conduction band). The *zero bandgap* behavior of the minority electrons converts the *halfmetallic ferrimagnet* into a *spin gapless semiconductor*. The magnetic moment is calculated to be $2 \mu_B$, as observed experimentally (see

below). The site-resolved spin magnetic moments are approximately $m_{\text{Mn}(4a)} = -2\mu_B$, $m_{\text{Co}(4b)} = +1\mu_B$, and $m_{\text{Mn}(4c)} = +3\mu_B$, confirming a ferrimagnetic character with antiparallel coupling of the moments at the neighboring Mn sites. In the following, it will be shown that various extraordinary physical properties are in agreement with the proposed behavior of a *spin gapless semiconductor*.

Polycrystalline Mn_2CoAl was prepared by arc melting. The resulting ingots were annealed at different temperatures under argon in quartz ampules. The annealing was followed by fast cooling to 273 K (quenching in ice-water). The crystalline structures, homogeneities, and compositions of the samples were checked by X-ray diffraction (XRD) and energy-dispersive X-ray (EDX) spectroscopy. No impurities or inhomogeneities were detected by EDX. Transport measurements were performed using a physical properties measurement system (PPMS; Quantum Design). For transport measurements, samples of $(2 \times 2 \times 8) \text{ mm}^3$ were cut from the ingots. The temperature was varied from 1.8 K to 350 K. The Hall effect of the compound was measured in the temperature range from 5 K to 300 K in magnetic induction fields from -9 to +9 T. The Hall coefficient was calculated from the slope of the measured Hall coefficient R_H . The carrier concentration $n = 1/eR_H$ was extracted from R_H using a single-band model [12] (e is the elementary electronic charge). The temperature dependence of the magnetization was measured from 4.8 K to 800 K using a magnetic properties measurement system (MPMS; Quantum Design). For these measurements, small sample pieces of approximately 8 mg were used. The experiments on Mn_2CoAl confirmed that it crystallizes in the expected crystalline structure. Powder XRD revealed single-phase samples with the Li_2AgSb structure and a lattice parameter of $a = 5.798 \text{ \AA}$ for the post-annealed samples. The saturation magnetic moment is $2 \mu_B$ at low temperature ($T < 5 \text{ K}$) (see inset b in Figure 5) and the compound has a Curie temperature of 720 K (Figure 5c).

The temperature dependences of the electrical conductivity $\sigma(T)$, Seebeck coefficient $S(T)$, and carrier concentration $n(T)$ of Mn_2CoAl are shown in Figure 3. The conductivity $\sigma(T)$ clearly exhibits non-metallic behavior, and is of semiconducting type: it increases with increasing temperature and a value of about 2440 S/cm is obtained at 300 K. As shown in Figure 3(b), the Seebeck coefficient $S(T)$ nearly vanishes in the temperature range from 5 K to 150 K and adopts a very low value of only about $2 \mu\text{V/K}$ at 300 K. Measurement of the Hall coefficient shows a very low carrier concentration of only $2 \times 10^{17} \text{ cm}^{-3}$ at 300 K. It is also nearly constant with temperature and approaches a value as low as $1.3 \times 10^{17} \text{ cm}^{-3}$ at 2 K.

The linear temperature coefficient of the resistivity is $-1.4 \times 10^{-9} \Omega\text{-m/K}$ and nearly independent of temperature up to 300 K. This behavior is remarkable and not

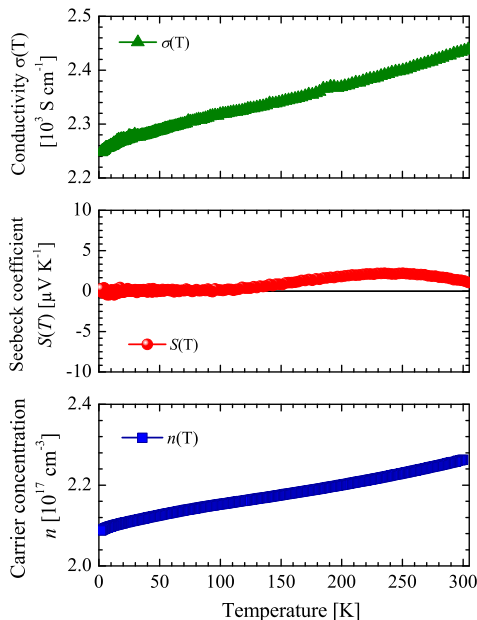


FIG. 3. Temperature dependences of conductivity $\sigma_{xx}(T)$, Seebeck coefficient $S(T)$, and carrier concentration $n(T)$ of Mn_2CoAl .

comparable to those of regular metals or semiconductors, which exhibit exponential increases or decreases in conductivity. As Mn_2CoAl is a well-ordered compound without antisite disorder, this behavior cannot be attributed to impurity scattering. A similar, linear behavior of the resistance was also reported for halfmetallic ferromagnets, but only at low temperatures [13]. The resistivity in those metallic systems ($< 0.5 \mu\Omega\cdot\text{m}$ for PtMnSn) is, however, three orders of magnitude lower than that of Mn_2CoAl ($\approx 400 \mu\Omega\cdot\text{m}$). The temperature-independent charge-carrier concentration is typical for gapless systems [5]. The value observed here is of the same order as that observed for HgCdTe ($10^{15} - 10^{17} \text{ cm}^{-3}$) and considerably lower than that for Fe_2VAl (10^{21} cm^{-3}) [14], a proposed semiconducting Heusler compound. Also, for gapless systems, the Seebeck effect is expected—as observed here—to vanish over a wide range of temperatures as a result of electron and hole compensation.

So far, the electronic transport properties, together with the predicted and measured magnetic moment of $2 \mu_B$, support the view that Mn_2CoAl is a spin gapless semiconductor. To investigate further transport properties of the spin gapless state, the magnetoresistance (MR) and anomalous Hall conductivity of Mn_2CoAl were measured.

The results of the MR measurements at different temperatures are displayed in Figure 4, and show a remarkable effect. Above 200 K, the MR is low and exhibits a negative, saturating dependence on the applied magnetic field. At lower temperatures, the MR becomes positive

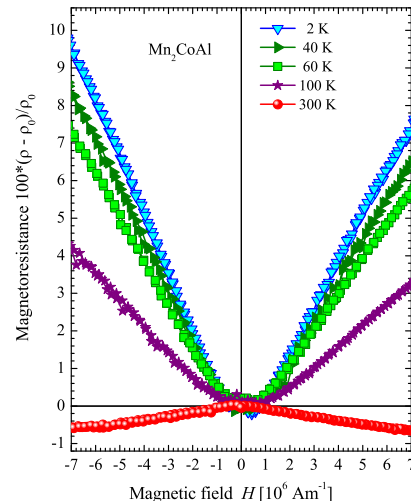


FIG. 4. Magnetoresistance of Mn_2CoAl measured at different temperatures.

and reaches a value of about 10% at 2 K for an induction field of 9 T. The low-temperature MR is clearly non-saturating and nearly linear, even in high fields. Above 1 T, its derivative has an approximately constant value of 10^{-4} T^{-1} at 2 K. A change of sign appears at around 150 K, where the Seebeck effect vanishes, and remains the same at lower temperatures. Various gapless semiconductors have already been shown to exhibit quantum linear MR [15] in very small transverse magnetic fields. For the present compound, and for spin gapless materials in general, the behavior in low fields becomes more complicated as a result of the influence of the ferrimagnetic order and the non-saturated magnetization in low fields. The MR changes sign at low fields, as seen from Figure 4; an appropriate theory is needed to describe the MR in spin gapless systems.

The anomalous Hall conductivity $\sigma_{xy} = \frac{\rho_{xy}}{\rho_{xx}}$ was extracted from the magnetic-field-dependent transport measurements to disentangle the low-field behavior in more detail. The result is shown in Figure 5. $\sigma_{xy}(H)$ follows the field dependence of the magnetization $m(H)$ (inset b of Figure 5). The anomalous Hall conductivity σ_{xy0} has a very low value of 22 S/cm at 2 K. This value is about 20 to 100 times smaller than those of other halfmetallic Heusler compounds [16].

The anomalous Hall effect was calculated using the Berry-phase approach [10] in order to explain its extraordinarily small value. The result of the calculation is shown in Figure 6. The symmetry of the Berry curvature $\Omega_z(\mathbf{k})$ in a plane of the Brillouin zone is clearly visible. This pattern symmetry is different from the patterns of regular ferromagnets (e.g., compare Fe [17]). Moreover, it is easily seen that the pattern for momentum vectors with the opposite sign (here at $k_z = \pm 0.25$) is nearly anti-

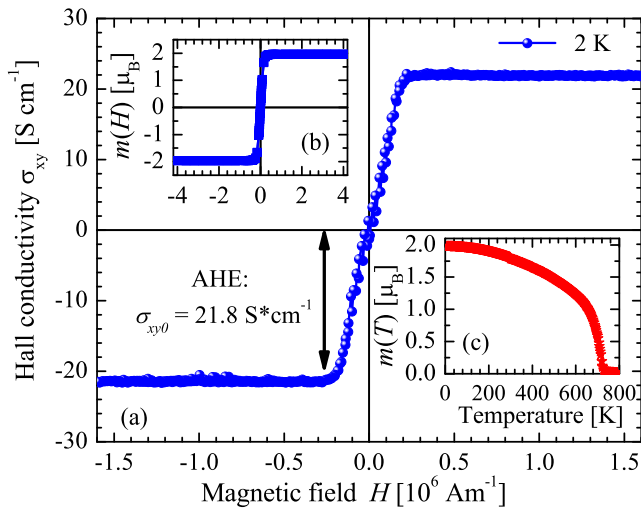


FIG. 5. Magnetic properties and anomalous Hall effect of Mn_2CoAl .

The Hall conductivity σ_{xy} is shown as a function of the applied magnetic field. The anomalous Hall effect is defined by the difference between σ_{xy} values in zero and saturation fields (≈ 0.3 T). Inset (a) shows the hysteresis $m(H)$ measured at 2 K. Inset (b) shows the temperature dependence of the magnetization $m(T)$ measured in a field of 1 T.

symmetric. The anomalous Hall conductivity is given by a Brillouin zone integral over the Berry curvature $\Omega_z(\mathbf{k})$ over all occupied states[17]:

$$\sigma_{xy} = \frac{e^2}{h} \int \frac{d\mathbf{k}}{(2\pi)^d} \Omega_z(\mathbf{k}) f(\mathbf{k}), \quad (1)$$

where $f(\mathbf{k})$ is the Fermi distribution function (at $T = 0$) and the dimension $d = 3$. This makes clear that the nearly vanishing anomalous Hall effect of Mn_2CoAl arises from the *antisymmetry* of the Berry curvature for k_z vectors of opposite sign. Indeed, a numerical integration of equation (1) gives $\sigma_{xy} = 3$ S/cm, which is lower than the experimental value. This small value comes from positive and negative contributions of about 150 S/cm each. The small switching field used in the experiment could therefore account for the difference between the calculated and experimental values.

Ab initio calculations suggested that the Heusler compound Mn_2CoAl is a good candidate for spin gapless semiconductivity. This unique class of materials will have a considerable impact on the field of spintronics as it opens up new and advanced possibilities for physical phenomena and devices based on spin transport. In spin gapless materials, only one spin channel contributes to the transport properties, whereas the other spin channel allows for tunable charge-carrier concentrations. In the present work, Mn_2CoAl was synthesized. Its crystalline structure is of the inverse Heusler type. The saturation magnetic moment is $2 \mu_B$ at 5 K and the Curie

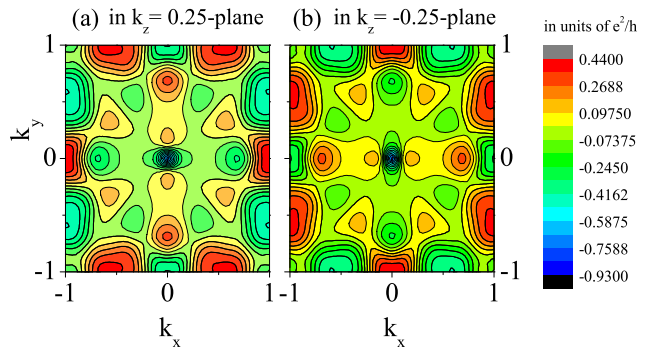


FIG. 6. Berry curvature in the $k_z = 0.25$ plane (a) and $k_z = -0.25$ plane (b) for Mn_2CoAl .

temperature of 720 K makes it suitable for applications. It has been shown by experiments and calculations that Mn_2CoAl is a spin gapless semiconductor with nearly temperature-independent, low conductivity of the order of 2×10^5 S/m, and a low charge-carrier concentration of the order of 10^{17} cm^{-3} , as well as a vanishing Seebeck coefficient. The temperature dependence of the MR is non-trivial. In high fields, it is positive, nearly linear, and non-saturating, with a value of 10% at 2 K in a magnetic field of 9 T. At temperatures above 150 K, it is negative and saturating, with low values. Berry curvature calculations were used to explain the low value of the anomalous Hall effect of 22 S/cm at 2 K.

The authors thank W. Schnelle (MPI, Dresden) for performing part of the transport measurements. This work was financially supported by the *Deutsche Forschungs Gemeinschaft* DfG (projects TP 1.2-A and TP 2.3-A of Research Unit FOR 1464 *ASPIMATT*).

* fecher@cpfs.mpg.de

- [1] X. L. Wang, Phys. Rev. Lett. **100**, 156404 (2008).
- [2] R. A. d. Groot, F. M. Müller, P. G. v. Engen, and K. H. J. Buschow, Phys. Rev. Lett. **50**, 2024 (1983).
- [3] S. Wurmehl, H. C. Kandpal, G. H. Fecher, and C. Felser, J. Phys.: Condens. Matter **18**, 6171 (2006).
- [4] H. v. Leuken and R. A. d. Groot, Phys. Rev. Lett. **74**, 1171 (1995).
- [5] I. M. Tsidilkovski, *Electron Spectrum of Gapless Semiconductors*, Springer Series in Solid-State Sciences, Vol. 116 (Springer, 1996).
- [6] S. H. Groves, R. N. Brown, and C. R. Pidgeon, Phys. Rev. **161**, 779 (1967).
- [7] S. Murakami, N. Nagaosa, and S.-C. Zhang, Phys. Rev. Lett. **93**, 156804 (2004).
- [8] C. L. Kane and E. J. Mele, Phys. Rev. Lett. **95**, 146802 (2005).

- [9] A. R. Williams, J. Kübler, and J. Gelatt, C. D., Phys. Rev. B **19**, 6094 (1979).
- [10] J. Kübler and C. Felser, Phys. Rev. B **85**, 012405 (2012).
- [11] G. D. Liu, X. F. Dai, H. Y. Liu, J. L. Chen, Y. X. Li, G. Xiao, and G. H. Wu, Phys. Rev. B **77**, 014424 (2008).
- [12] D. M. Rowe, *Thermoelectrics Handbook: Macro to Nano*, 1st ed. (CRC/Taylor & Francis, Boca Raton, 2006).
- [13] J. S. Moodera and D. M. Mootoo, J. Appl. Phys. **76**, 6101 (1994).
- [14] V. I. Okulov, V. E. Arkhipov, T. E. Govorkova, A. V. Korolev, and K. A. Okulova, Low Temp. Phys. **33**, 692 (2007).
- [15] A. A. Abrikosov, Phys. Rev. B **58**, 2788 (1998).
- [16] D. Bombor, C. G. F. Blum, O. Volkonskiy, S. Rodan, S. Wurmehl, C. Hess, and B. Büchner, arXiv:1207.6611 [cond-mat.str-el] (2012).
- [17] Y. Yao, L. Kleinman, A. H. MacDonald, J. Sinova, T. Jungwirth, D.-s. Wang, E. Wang, and Q. Niu, Phys. Rev. Lett. **92**, 037204 (2004).